MiR-221 and miR-222 regulate cell cycle progression and affect chemosensitivity in breast cancer by targeting ANXA3

JU-YEON KIM[1], EUN JUNG JUNG[2], JAE-MYUNG KIM[1], YOUNGSIM SON[1], HAN SHINE LEE[2], SEUNG-JIN KWAG[1], JI-HO PARK[1], JIN-KYU CHO[1], HAN-GIL KIM[1], TAEJIN PARK[2], SANG-HO JEONG[2], CHI-YOUNG JEONG[1] and YOUNG-TAE JU[1]

[1]Department of Surgery, Gyeongsang National University School of Medicine and Gyeongsang National University Hospital, Jinju, Gyeongsang 52727; [2]Department of Surgery, Gyeongsang National University School of Medicine and Gyeongsang National University Changwon Hospital, Changwon, Gyeongsang 51472, Republic of Korea

Received July 25, 2022; Accepted December 15, 2022

DOI: 10.3892/etm.2023.11826

Abstract. Breast malignancy remains one of the most common causes of cancer-associated mortalities among women. MicroRNA (miR)-221 and miR-222 are homologous miRs and have a substantial impact on cancer progression. In the present study, the regulatory mechanisms of miR-221/222 and its target annexin A3 (ANXA3) in breast cancer cells were investigated. Breast tissue samples were collected to evaluate the expression patterns of miR-221/222 levels in breast cancer cell lines and cancer tissues according to clinical characteristics. The levels of miR-221/222 were increased or decreased in cancer cell lines compared with normal breast cell lines according to cell line subtype. Subsequently, the changes in the progression and invasion of breast cancer cells were investigated using cell proliferation, invasion assay, gap closure and colony formation assays. Western blotting of cell cycle proteins and flow cytometry were performed to evaluate the possible pathway of miR-221/222 and ANXA3 axis. Chemosensitivity tests were performed to explore the suitability of the miR-221/222 and ANXA3 axis as a therapeutic target in breast cancer. The expression levels of miR-221/222 were associated with aggressive characteristics of breast cancer subtypes. Cell transfection assay demonstrated the regulation of breast cancer proliferation and invasiveness by miR-221/222. MiR-221/222 directly targeted the 3'-untranslated region of ANXA3 and suppressed the expression of ANXA3 at the mRNA and protein levels. In addition, miR-221/222 negatively regulated cell proliferation and the cell cycle pathway in breast cancer cells by targeting ANXA3. In combination with adriamycin, downregulation of ANXA3 may sensitize adriamycin-induced cell death to induction of persistent G_2/M and G_0/G_1 arrest. Decreased expression of ANXA3 through increased expression of miR-221/222 reduced breast cancer progression and increased the effectiveness of the chemotherapy drug. The present results indicated the miR-221/222 and ANXA3 axis to be a possible novel therapeutic target for the treatment of breast cancer.

Correspondence to: Professor Eun Jung Jung, Department of Surgery, Gyeongsang National University School of Medicine and Gyeongsang National University Changwon Hospital, 11 Samjeongja-ro, Seongsan, Changwon, Gyeongsang 51472, Republic of Korea
E-mail: drjej@gnu.ac.kr

Key words: breast neoplasm, microRNA-221, microRNA-222, annexin A3, chemotherapy

Introduction

Breast cancer is a common malignant disease that affects women throughout the world and, despite the advancements in innovative systemic and local therapies, a substantial number of women continue to develop refractory breast cancer during treatment, eventually resulting in recurrence (1). Breast cancers are heterogeneous and can be classified into several subtypes according to distinct gene expression profiles (2). There is also a significant degree of variation in the response to treatment, which is the focus of basic and translational studies in this field. To develop more effective treatments, a comprehensive understanding of the molecular biological mechanisms involved in breast tumor development and aggressiveness is warranted.

MicroRNAs (miRNAs/miRs) are non-coding, single-stranded RNA molecules that influence target gene expression by posttranscriptional processing (3). Numerous studies have focused on the relationship between miRNAs and cancer pathology. Studies have shown that miRNAs are involved in tumor development, and are differentially expressed according to the tumor molecular subtype, thus the expression profiles of specific miRNAs can be used to classify tumor malignancies (4,5). MiR-221 and miR-222 are clustered miRNAs that, having the same seed sequence, can together regulate target genes and are encoded on chromosome Xp11.3, which is a key modulator in the regulation of a wide range of malignancies (6). Studies have revealed that basal-like breast cancer has a higher expression level of miR-221/222 compared with luminal breast cancer (7,8). MiRNA can function differently depending on the target mRNAs. Several studies focused on tumor progression, invasion, metastasis and drug resistance

in relation to miRNAs and target mRNAs expressed in cancer (6,9). For example, previous studies revealed the function of miR-221/222 in cancer stem cell-like properties, tumor aggressiveness and chemosensitivity in various types of cancer, including different types of breast cancers (8-12).

Annexin A3 (ANXA3) belongs to the annexin family of proteins. Members of this calcium-dependent phospholipid-binding protein family are involved in cancer formation and progression, as well as signal transduction and cellular growth regulation pathways (13). ANXA3 expression is connected to tumor growth and poor prognosis, as silencing ANXA3 lowers breast cancer cell aggressiveness by decreasing cell proliferation, migration, colony formation and invasion (14). A recent study also revealed that the decreased expression of ANXA3 mediated by miR-125 can limit lung cancer cell growth and invasion while promoting apoptosis (15).

The present study used web-based tools to predict the miRNAs targeting ANXA3 and revealed a relationship between miR-221/222 and ANXA3. Moreover, the mechanism and functional role of the miR-221/222 and ANXA3 axis in breast cancer progression and its effects on breast cancer treatment were further investigated.

Materials and methods

Tissue samples. The Institutional Review Board of Gyeongsang National University Hospital approved the collection of breast tissue samples (approval no. GNUHIRB2009-54). The cases for which the invasive tumor size was too small or scattered (largest diameter <0.2 cm), or for which the tissue collection might later interfere with the final pathological diagnosis, were excluded. In addition, male breast patients and patients who underwent neoadjuvant chemotherapy were also excluded. After obtaining written informed consent from patients, a total of 60 patients who underwent curative surgery for invasive breast cancer between August 2007 and December 2011 were randomly selected from the database of the Gyeongsang National University Hospital (Jinju, Korea). Of the 60 patients initially selected for the study, two were excluded since one presented with squamous cell carcinoma and the other with lymphoma. Of the remaining 58 patients (age 31-76 years old, mean 58 years), 22, 23 and 13 patients were TNM stage I, II and III (American Joint Committee on Cancer, 8th edition) (16), respectively. The breast cancer samples as well as their adjacent normal breast tissues (~1 cm from the cancer free resection margin) were resected during the operation and stored at -70˚C for further analysis. All obtained samples were determined to be invasive breast cancer by a pathologist, independent of the present study. Pathology data and the presence of recurrence were reviewed.

For the survival analysis, the Kaplan-Meier Plotter software (http://kmplot.com/analysis/) was used to compare ANXA3 groups in breast cancer using the mRNA gene chip tool. ANXA3 groups were divided into high and low according to auto select best cutoff.

Cell preparation and transfection. The Korean Cell Line Bank provided the human breast cancer and normal breast epithelial cell lines used in the present study (MCF-7, T47D, ZR-75-1, SK-BR-3, HCC-1954, MDA-MB 231, HCC-70 and MCF-10A). These cell lines were all grown in RPMI-1640 medium (Gibco; Thermo Fisher Scientific, Inc.) with 10% fetal bovine serum (FBS) (Gibco; Thermo Fisher Scientific, Inc.), 100 U/ml penicillin and 100 g/ml streptomycin at 37˚C in a humidified incubator with 5% CO_2. The main cell functional experiments were conducted by selecting two representative cell lines: MCF-7 (luminal A subtype); and MDA-MB 231(basal-like subtype). For transient transfection, hsa-miR-221-3p mimic (5'-AGCUACAUUGUCUGCUGGGUUUC-3', cat. no. PM10337), has-miR-222-3p mimic (5'-AGCUACAUC UGGCUACUGGGU-3', cat. no. PM11376), hsa-miR-221-3p inhibitor (5'-AGCUACAUUGUCUGCUGGGUUUC-3', cat. no. AM10337), hsa-miR-222-3p inhibitor (5'-AGCUACACC UGGCUACUGGGU-3', cat. no. AM11376), the scrambled negative control (SCR; cat. no. AM17110), and anti-miR negative control (cat. no. AM17010) were purchased from Ambion (Thermo Fisher Scientific, Inc.). The non-targeting small interfering (si)RNA negative control (siCTL; cat. no. sc-37007) and ANXA3 targeting siRNA (sc-89288) were purchased from Santa Cruz (Santa Cruz Biotechnology, Inc.). The ANXA3 targeting siRNA used was a pool of 3 different siRNAs; 5'-CAGCAGUCUUUGAUGCAAA-3', 5'-GGAGAU GACUGAACCAAGA-3' and 5'-GCAACUACUAUCCAA CUUA-3'. The pCMV6-myc-DDK-tagged human ANXA3 (oeANXA3; cat. no. RS201540) and pCMV Entry-myc-DDK empty vector (oeCTL; cat. no. RS100001) were purchased from OriGene Technologies, Inc and used as overexpression and negative control vectors. MCF-7 and MDA-MB-231 cells were seeded into six-well plates with $3x10^5$ cells per well for 48-72 h at 37˚C. Cells were transfected with the indicated miRNAs (50-100 nM/well), anti-miRNAs (50-100 nM/well), siANXA3 (50-100 nM/well) and oeANXA3 (0.25-0.5 μg/well) at 37˚C using serum-free RPMI 1640 medium (Gibco; Thermo Fisher Scientific, Inc.). Transient transfections were accomplished using the Lipofectamine 2000® reagent in compliance with the manufacturer's instructions (Invitrogen; Thermo Fisher Scientific, Inc.). After replacing the total fresh medium within 48-72 h, the following experiments were performed. Reverse transcription-quantitative polymerase chain reaction (RT-qPCR) and western blotting were performed to assess transfection efficiency.

Western blotting. MCF-7 and MDA-MB-231 cells were transfected with miR-221/222, anti-miR-221/222, siANXA3, oeANXA3 and controls, followed by incubation for 48-72 h at 37˚C. Cells were lysed using RIPA lysis and extraction buffer (Thermo Fisher Scientific, Inc.) containing protease inhibitors (cat. no. P3100; GenDEPOT, LLC). The total protein from each sample was quantified using the BCA assay method (Thermo Fisher Scientific, Inc.). Total protein (20 μg/lane) was separated via sodium dodecyl sulfate-polyacrylamide gel electrophoresis on a 10-15% gel and transferred onto a polyvinylidene difluoride membrane (iBlot PVDF Regular Stacks; Invitrogen; Thermo Fisher Scientific, Inc.). Membranes were blocked in tris-buffered saline and Tween 20 (0.1% v/v) supplemented with 5% non-fat dry milk at room temperature for 1 h. Membranes were incubated with primary antibodies at 4˚C overnight. After washing three times, the membranes were incubated with a suitable secondary antibody at room temperature for 1 h and

visualized with ECL detection reagent (Clarity™ Western ECL Substrate; Bio-Rad Laboratories, Inc.). Signal intensity was semi-quantified using Image Lab software version 5.2.1 (Bio-Rab Laboratories, Inc.). The primary antibodies were: Anti-annexin A3 (1:1,000; cat. no. ab33068; Abcam); anti-cyclin D1 (1:500; cat. no. sc-20044; Santa Cruz Biotechnology, Inc.); anti-CDK4 (1:500; Santa Cruz Biotechnology, Inc.; cat. no. sc-56277); anti-cyclin B1 (1:500; cat. no. sc-245; Santa Cruz Biotechnology, Inc.); anti-cyclin A (1:500; cat. no. sc-274682; Santa Cruz Biotechnology, Inc.); anti-α tubulin (1:1,000; cat. no. sc-5286; Santa Cruz Biotechnology, Inc.); anti-β-Actin (1:1,000; cat. no. sc-47778; Santa Cruz Biotechnology, Inc.); apoptosis western blot cocktail (1:250; cat. no. ab136812; Abcam); and total poly ADP ribose polymerase (1:1,000; cat. no. 9542; Cell Signaling Technology, Inc.). The secondary antibodies were: Goat anti-rabbit IgG (H+L) antibody (1:2,000; cat. no. 31460; Thermo Fisher Scientific, Inc.), goat anti-mouse IgG (H+L) antibody (1:2,000; cat. no. 31430; Thermo Fisher Scientific, Inc.).

RT-qPCR. Total RNA was isolated from cell lines (MCF-7, T47D, ZR-75-1, MDA-MB-231 and HCC-70) and normal breast epithelial cell line (MCF-10A) using QIAzol® lysis reagent (Qiagen, Inc.), according to the manufacturer's instructions. Total RNA was reverse transcribed into cDNA using the SuperScript™ III cDNA synthesis kit (Invitrogen; Thermo Fisher Scientific, Inc.) and the Tagman™ MicroRNA Assay (cat. no. 4427975; Applied Biosystems; Thermo Fisher Scientific, Inc.) was added to this reaction to synthesis the cDNA for specific miRNA (hsa-miR-221 (assay ID, 000524), hsa-miR-222 (assay ID, 002276) and U6 small nuclear RNA (assay ID, 001973)). The reverse transcription PCR conditions were performed at 24˚C as the priming stage for 5 min, 46˚C as the reverse transcription (RT) step for 20 min and 95˚C as RT inactivation stage for 1 min. Subsequently, quantitative real-time PCR was performed in PCR mixture using the 20 X TaqMan miR Asaasy and 2X TaqMan™ Universal PCT Master Mix (Applied Biosystem, Calsabd, cat. No. 4304437) according to the manufacturer's instructions. RT-qPCR conditions were as follows: initial denaturation at 50˚C for 2 min and 95˚C for 10 min as the hold stage; 40 cycles at 95˚C for 15 sec and 60˚C for 1 min. The assays used were as follows; hsa-miR-221-3p (assay ID, 000524); hsa-miR-222-3p (assay ID, 002276); and U6 small nuclear RNA (assay ID, 001973), all TaqMan miR assays were purchased from Applied Biosystems (Thermo Fisher Scientific, Inc.). The relative mRNA expression levels of miR-221 and miR-222 were measured using a ViiA™ 7 Real-Time PCR System (Applied Biosystems; Thermo Fisher Scientific, Inc.). Data were analyzed according to the comparative threshold cycle value $2^{-\Delta\Delta Cq}$ method (17).

Dual-luciferase reporter assay. The miRNAs interacting with ANXA3 were investigated through web-based prediction tools for interactions between miRNAs and target genes, such as miTarget (www.Mitarget.org), PicTar (www.Genome.ucsc.edu) and miRanda (https://tools4mirs.org/software/target_prediction/Miranda/), and miR 221/222 resulted suitable for the present study. The 3' untranslated region (3'-UTR) of the human ANXA3 gene insert was amplified from genomic DNA and cloned into the Xba1/BamHI sites of the pGL3 promoter vector (Promega Corporation). The ANXA3 3'-UTR-mutant construct was generated using a QuikChange® II XL Site-Directed Mutagenesis kit (Stratagene; Agilent Technologies, Inc.). Sequencing was performed using MACROGEN (Capillary Electrophoresis sequencing; CES) to identify the wild-type and mutant sequences. For luciferase analysis, MCF-7 and MDA-MB-231 cells were seeded into 24-well plates at $5x10^4$ cells/well, incubated for 24 h at 37˚C and then co-transfected using Lipofectamine 2000® (Invitrogen; Thermo Fisher Scientific, Inc.). with 400 ng of ANXA3 3'-UTR wild-type or mutated plasmid, 80 ng of pRL-TK *Renilla* luciferase reporter (Promega Corporation) and 50 nM of control miR (AM 17110) or pre-miR-221 (5'-AGCUACAUUGUCUGC UGGGUUUC-3', cat. no. PM10337; Ambion; Thermo Fisher Scientific, Inc.) and pre-miR-222 (5'-AGCUACAUCUGG CUACUGGGU-3', cat. no. PM11376; Ambion; Thermo Fisher Scientific, Inc.) for 48 h at 37˚C. Transfections were performed using Lipofectamine 2000® (Invitrogen; Thermo Fisher Scientific, Inc.). After 48 h, luciferase activity was measured using the Dual-Luciferase® Reporter Assay System (Promega Corporation). The luminescent signal was quantified with a luminometer (Glomax; Promega Corporation) and the activity of the firefly luciferase was normalized to the signal of the *Renilla* luciferase reporter activity.

Cell proliferation assay. The percentage of viable cells was determined using 3-(4,5-dimethylthiazol-2-yl)-2 and 5-diphenyl-tetrazolium bromide (MTT; Sigma-Aldrich; Merck KGaA) to assess cell proliferation. A total of $2x10^4$ cells/well were seeded into 24-well plates and subsequently transfected, according to the aforementioned method, with the control miR, miR-221, miR-222, anti-miR-221, anti-miR-222, siANXA3 or oeANXA3. Cells were incubated with MTT and dimethyl sulfoxide (DMSO) was added to each culture. DMSO was used to dissolve the purple formazan. The optical density was measured at 570 nm using a VersaMax™ ELISA Microplate Reader (Molecular Devices, LCC) at 0, 24, 48, 72 and 96 h of incubation. Each experiment was performed three times.

Invasion assay. A Matrigel-based Transwell system (8-mm pore size polycarbonate membrane; Corning, Inc.) was used to examine the invasiveness of transfected cells. The Transwell inserts were covered with a homogenous layer of BD Matrigel™ Basement Membrane Matrix (BD Biosciences) and incubated for 4 h at 37˚C in 24-well plates containing RPMI-1640 medium per 10-20 μl/well. Then, $0.3\text{-}1.0x10^5$ cells/well in 250.0 μl serum-free medium were plated into the upper chamber and allowed to invade for 24-72 h at 37˚C. A total of 650.0 μl of RPMI 1640 medium containing 10% FBS (Gibco; Thermo Fisher Scientific, Inc.) was plated in the lower chamber. The residual medium on the top insert was removed after the incubation time and non-invading cells on the upper surface were gently scraped with a brush. The migrating cells to the lower chambers were fixed in a fixing solution (4% formaldehyde in PBS with 0.1% Tween-20) at room temperature for 20 min after being washed twice with PBS. The cells were then stained for 10 min at 37˚C with 4',6-diamidino-2-phenylindole solution (Sigma-Aldrich; Merck KGaA) and photographed using a microscope Nikon ECLIPSE Ti inverted light microscope (Nikon Corporation)

at 100x or 200x magnification. Subsequently, the number of invasive cells was by three fields per chamber using Image J software 1.52d (National Institutes of Health).

Gap closure assay. The two-well silicone insert (Ibidi GmbH) was utilized to perform the gap closure experiment. Adhesive inserts with sticky floors were pasted onto six-well plates before performing the experiments. After transfection, the MCF-7, MDA-MB-231 cells (5.0-7.0x10^5 cells per each side of the insert) were reseeded into a two-well silicone insert with 70.0 μl of cell suspension and cultured for 24 h at 37˚C to create a 500 μm gap in a confluent cell monolayer. The inserts were then gently removed with sterile tweezers and immediately taken under a microscope (Nikon ECLIPSE Ti inverted microscope; Nikon Corporation) to collect sample images at timepoint zero. The plates were rinsed several times in PBS and incubated with fresh RPMI 1640 medium containing 10% serum (Gibco; Thermo Fisher Scientific, Inc.) for 17 or 30 h at 37˚C. At different time points, the plates were taken under a Nikon ECLIPSE Ti inverted light microscope (magnification, 40x; Nikon Corporation). In the images taken using the microscope, the area of the gap was marked and assessed using ImageJ 1.52d (National Institutes of Health). Data were normalized to the mean value at time zero.

Colony forming assay. Transfected MCF-7 and MDA-MB-231 cells (2.0x10^2 cells/well) using the Lipofectamine 2000® reagent (Invitrogen; Thermo Fisher Scientific, Inc.) were plated into six-well plates and incubated at 37˚C for 10-15 days, with the medium replaced every three days, changing the medium every three days. Cells were rinsed in PBS, fixed in 100% methanol for 30 min at 4˚C and stained with crystal violet (1% w/v; Sigma-Aldrich; Merck KGaA) at room temperature for 1-3 h. The number of stained colonies (50 or more cells forming a colony with, diameter >200 μm) were scanned using a UMAX PowerLook 2100XL scanner (MagicScan software, version 4.5, UMAX) and then analyzed using Image J 1.52d (National Institutes of Health).

Flow cytometry cell cycling analysis. Transfected cells were treated with adriamycin for 48-72 h at 37˚C after transient transfection with siANXA3 and control siRNA. Sigma-Aldrich (Merck KGaA) provided the adriamycin (cat. no. 079M4765V) and DMSO (cat. no. D2650). After 5 min of exposure to 0.25% Trypsin-EDTA solution, cells were collected and centrifuged at 440 x g for 5 min at 4˚C, rinsed twice in cold PBS and fixed with ice-cold ethanol (70% w/w) at -20˚C for 3 h to overnight. Subsequently, cells were centrifuged at 440 x g for 5 min at 4˚C and were stained in the dark at room temperature for 30 min in PBS containing 0.1% Triton X-100, RNase A (10 g/ml; Fermentas; Thermo Fisher Scientific, Inc.) and propidium iodide (PI; 50 g/ml; Sigma-Aldrich; Merck KGaA) immediately prior to analysis. The flow cytometer LSRFortessaTM X-20 (BD Biosciences) was used to measure the cell cycle according to the manufacturer's instructions. Data analysis was performed using the BD FACSDiva™ software (version 8.0.3, BD Biosciences).

Apoptosis assay. Cells that had been transfected with siRNA were collected, washed twice with PBS and stained with the Annexin V-FITC Apoptosis Detection kit (BD Biosciences) to count the ratios of apoptotic cells, according to the manufacturer's instructions. Cells were resuspended in 100 μl 1X binding buffer [10 mM HEPES/NaOH (pH 7.4), 140 mM NaCl, 2.5 mM $CaCl_2$] after being rinsed with cold PBS. After that, 5 ml Annexin V-FITC and 5 μl PI were added to the cells and these were incubated at room temperature for 15 min in the dark. Subsequently, cells were added to 400 μl 1X binding buffer and flow cytometry (LSRFortessa™ X-20; BD Biosciences) was performed within 1 h. Data analysis was performed using the BD FACSDiva™ software (version 8.0.3, BD Biosciences).

Chemosensitivity. Cells were plated into 24-well plates and transfected with siANXA3 and control siRNA the next day. After 6 h of transfection, each adriamycin concentration was added with fresh complete medium and cultured for 48 h at 37˚C. Concentrations of adriamycin 5, 50, 100 and 200 nM were prepared in DMSO. After treatments, the cells were incubated with MTT solution (Sigma) for 3 h at 37˚C, the supernatant was removed, and 100% DMSO was added to dissolve the purple formazan crystals in the dark for 20 min at room temperature. Absorbance at 570 nm was recorded using a VersaMax™ ELISA Microplate Reader (Molecular Devices, LLC).

Statistical analysis. Data are presented as the mean ± standard deviation and all experiments were performed in duplicate for at least three independent experiments. GraphPad Prism 5 (version 5.04; GraphPad Software, Inc.) was used to perform paired two-tailed Student's t-test. Multiple comparison differences were analyzed using the paired Kruskal-Wallis test followed by Mann-Whitney U test for post-hoc comparisons in SPSS (version 21.0; IBM Corp.). $P<0.05$ was considered to indicate a statistically significant difference.

Results

The levels of miR-221 and miR-222 are related to breast cancer characteristics. The levels of miR-221 and miR-222 varied amongst breast cancer cell lines (Fig. 1A). The luminal type cancer cell lines (MCF-7, T47D and ZR-75-1) had lower levels whereas the basal type cancer cell lines (MDA-MB-231 and HCC-70) had significantly increased levels when compared with the normal breast epithelial cell line MCF-10A. Her-2 positive breast cancer cell lines, such as SK-BR-3 and HCC-1954, showed different expression levels. The expression of miR-221 and miR-222 was low in SK-BR-3. However HCC-1954 is a poorly differentiated breast cancer cell (18), so it may have had a significantly increased expression of miR-221/222 due to poor breast cancer characteristics. RT-qPCR was performed to assess the tissue levels of miR-221 and miR-222 in 58 patients with breast cancer. Similarly to the cell line results, the expression levels of miR-221 and miR-222 were different according to the cancer subtypes. Compared with adjacent normal tissues, tumor tissue levels of miR-221 and miR-222 were significantly downregulated in luminal A and luminal B types and were significantly upregulated in HER-2 and basal-like types (Fig. 1B). Notably, tumor tissue levels of miR-221 and miR-222 were significantly higher in patients who had lymph node metastasis and had experienced recurrence (Fig. 1C and D).

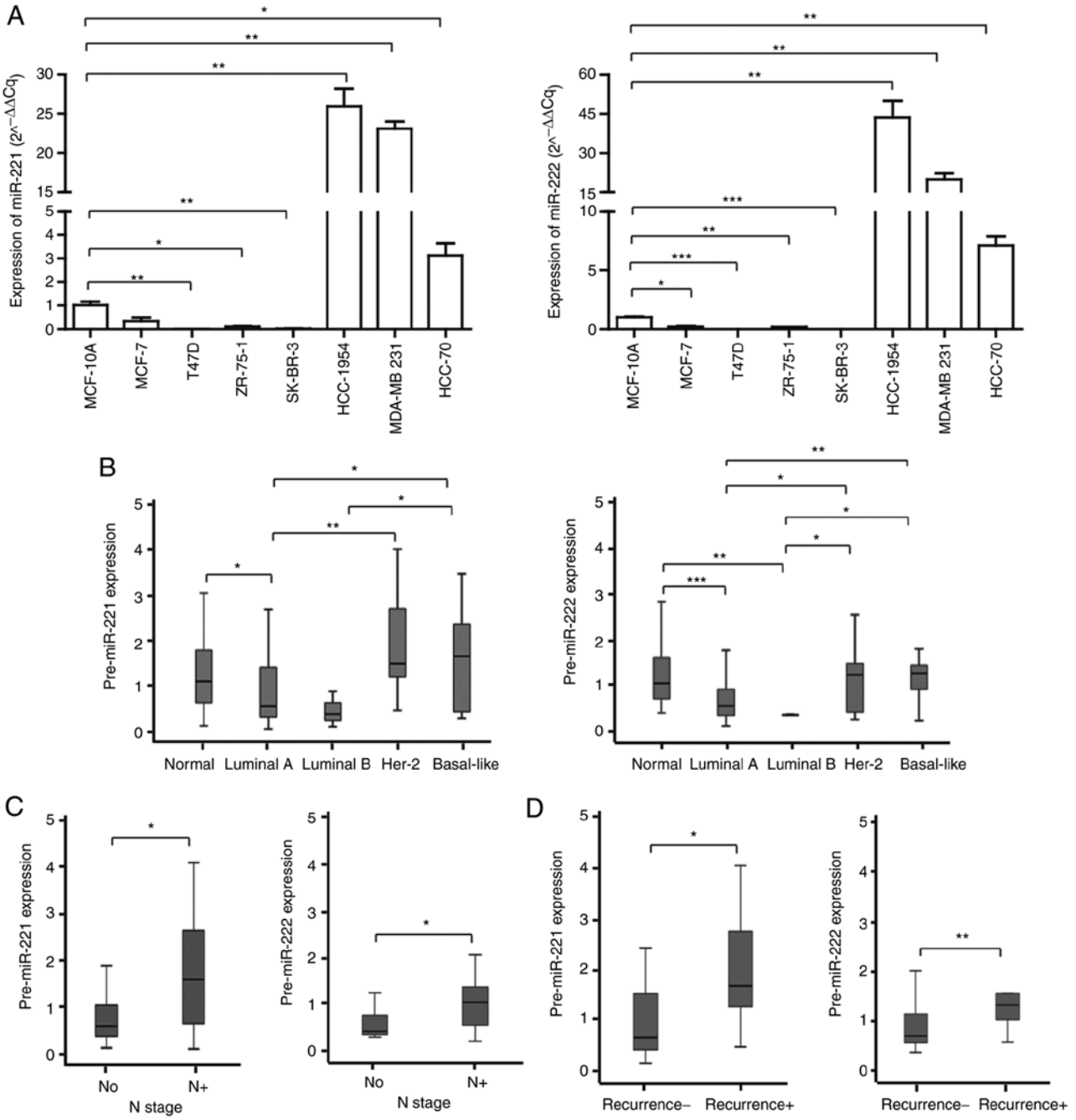

Figure 1. Expression patterns of miR-221 and miR-222 in breast cancer cell lines and tissues. (A) MiR levels in various breast cancer cell lines. (B) MiR levels in cancer tissues. (C) MiR levels in the lymph nodes of metastasis-negative (N0; n=36) or positive (N+; n=22) patients with breast cancer. (D) Cancer tissue miR levels in patients without disease-recurrence (recurrence-; n=44) or with disease recurrence (recurrence+; n=14). *P<0.05, **P<0.01 and ***P<0.001. MiR, microRNA.

Regulation of breast cancer proliferation and invasiveness by miR-221 and miR-222. Typical cell lines, such as MCF-7 and MDA-MB-231, were used to examine the biological role of miR-221 and miR-222. The control and pre-miR-221/222 were transfected into MCF-7 cells and expression of miR-221/222 was significantly upregulated compared with the control (Fig. 2A). Whereas anti-miR control and anti-miR-221/222 were transfected into MDA-MB-231 cells and expression of miR-221/.222 was significantly downregulated compared with the control (Fig. 3A). Cell proliferation, colony forming gap closure, and invasion assays were subsequently performed. MiR-221/222 overexpression significantly inhibited MCF-7 cell proliferation (61.0±0.1%; Fig. 2B), invasion (16.2±2.5%; Fig. 2C), gap closure (39.1±17.8%; Fig. 2D) and colony formation (34.3±18.5%; Fig. 2E). In MDA-MB-231 cell, the inhibition of miR-221/222 expression demonstrated a slight increase in cell proliferation rate (104.9±0.06%; Fig. 3B); however there was no statistical significance. In other functional studies, similar to the results of MCF-7, inhibition of miR-221/222 expression increased MDA-MB-231 cell invasiveness (mean; 223.9±8.8%; Fig. 3C), gap closure (162.5±19.6%; Fig. 3D) and colony formation (129.7±23.4%; Fig. 3E) with statistical significance. Overall, the present findings suggested that miR-221/222 was involved in the growth and progression of breast cancer.

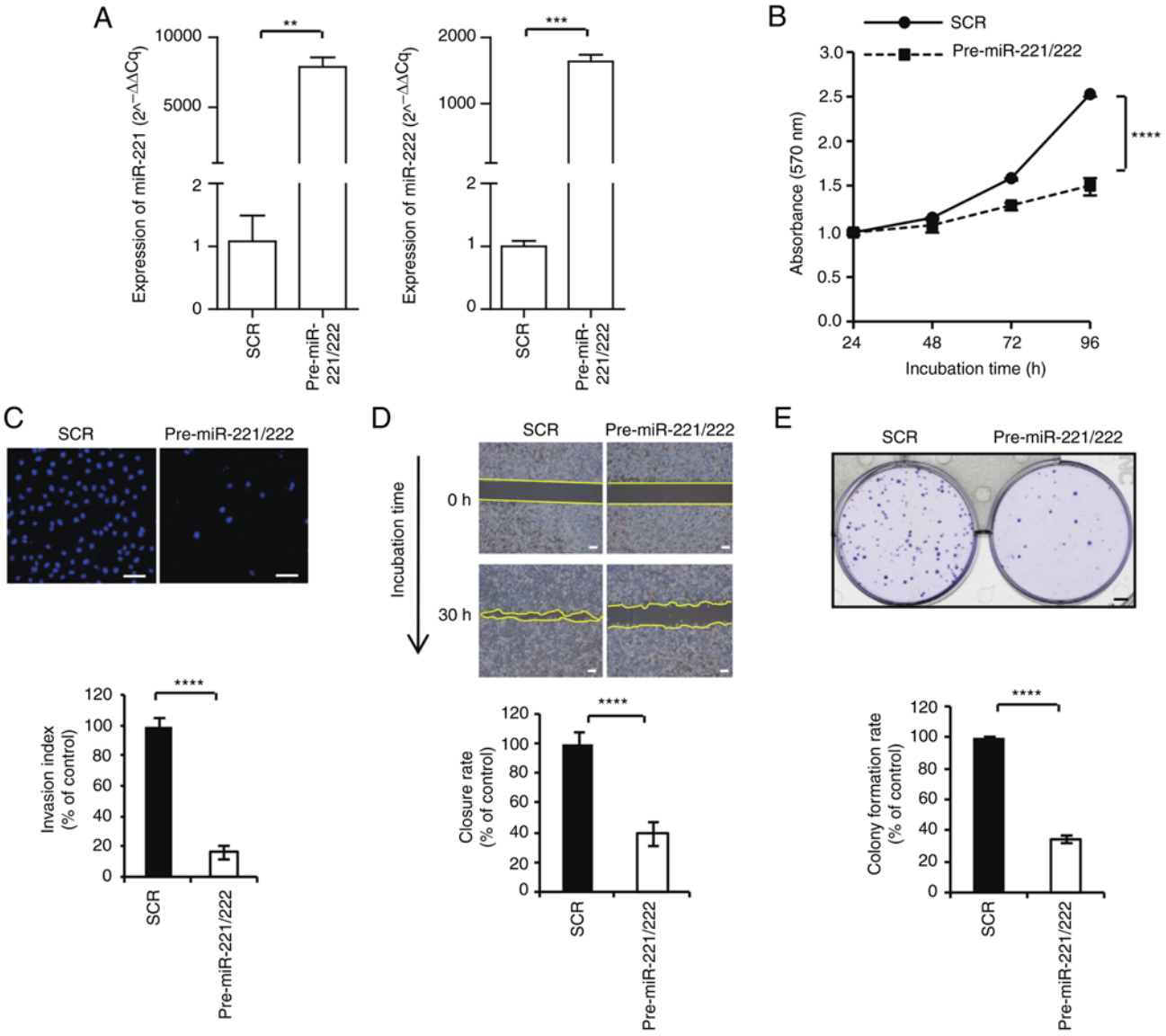

Figure 2. Inhibitory effect of miR-221/222 on MCF-7 cell proliferation, invasion, gap closure and colony formation. (A) MCF-7 cells were transfected with scrambled negative control, pre-miR-221/222, anti-miR control and anti-miR-221/222. The expression levels of miR-221 and miR-222 were determined via reverse transcription-quantitative PCR. (B) Cell proliferation assays were performed at 24, 48, 72 and 96 h after transfection. (C) Invasion activity was evaluated using Transwell assay (magnification, x100). (D) Gap closure assay. Microscopic examinations were performed 30 h after scratching the cell surface. (E) Cells were seeded and allowed to grow until visible colonies appeared. **P<0.01, ***P<0.001 and ****P<0.0001. SRC, scrambled negative control; miR, microRNA; SCR, scrambled.

ANXA3 is a direct target of miR-221 and miR-222. A dual-luciferase assay was performed on MCF-7 and MDA-MB-231 cells to investigate whether ANXA3 was a direct target of miR-221/222. The wild-type 3'-UTR or the mutant 3'-UTR missing the miR-221/222 binding region was used (Fig. 4A). In cells transfected with the luciferase gene with the wild-type 3'-UTR of ANXA3, luciferase activity was significantly decreased when miR-221/222 were overexpressed. By contrast, in cells expressing the mutant 3'-UTR, miR-221/222 transfection had no marked effect on luciferase activity (Fig. 4B). Western blotting showed that the overexpression of miR-221 and miR-222 resulted in significant ANXA3 downregulation in both cell lines, whereas anti-miR-221 and anti-miR-222 transfections resulted in ANXA3 upregulation in MCF-7 cell line (Fig. S1 and Fig. 4C). These findings revealed that ANXA3 was a direct target of miR-221 and miR-222 in breast cancer.

MiR-221/222 and ANXA3 axis regulates cell cycle-related proteins. Western blotting of cyclin D1 and CDK4 was used to study the relationship between cell cycle components. Combination with overexpression of miR-221/222, as well as the subsequent drop in the levels of ANXA3, led to a decrease in cyclin D1 and CDK4 expression compared with the ANXA3 overexpression group in the MCF-7 cell line (Fig. 5A and B). The cell proliferation assay corroborated this conclusion. The increase in cyclin D1 and CDK4 expression by overexpression of ANXA3 in the MCF-7 cell line (Fig. S2) increased cell proliferation, while the decrease in cell proliferation owing to the decrease in cyclin D1 and CDK4 expression by miR-221/222 transfection was confirmed [5.04±0.04 (oeANXA3) vs. 3.92±0.03 (oeANXA3 + miR-221/222) at 96 h timepoint; P<0.01; Fig. 5C]. Similarly, in the MDA-231 cell line, the inhibition of miR-221 and miR-222 increased

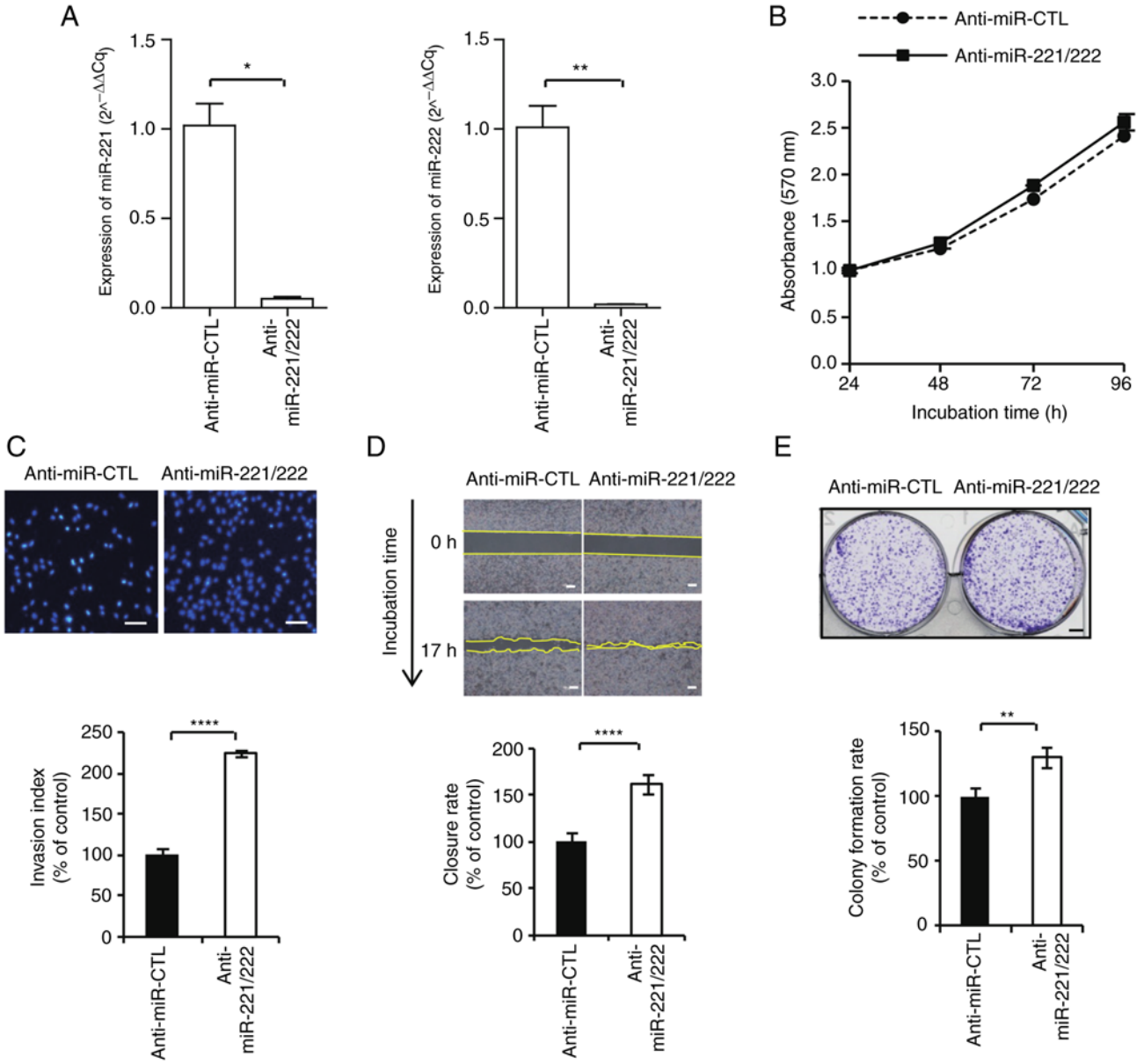

Figure 3. Inhibition of miR-221/222 promotes MDA-MB-231 cell proliferation, invasion, gap closure and colony formation. (A) MDA-MB-231 cells were transfected with scrambled negative control, pre-miR-221/222, anti-miR control and anti-miR-221/222. The expression levels of miR-22 and miR-222 were measured using reverse transcription-quantitative PCR. (B) Cell proliferation assays were performed at 24, 48, 72 and 96 h after transfection. (C) Invasion activity was evaluated using Transwell assay (magnification, x100). (D) Gap closure assay. Microscopic examinations were performed 17 h after scratching the cell surface. (E) Cells were seeded and allowed to grow until visible colonies appeared. *P<0.05, **P<0.01 and ****P<0.0001. miR, microRNA; SCR, scrambled.

cyclin D1 and CDK4 expression (Fig. 5D and E) while inhibition of ANXA3 showed inhibitory effect on cell proliferation by decreasing cyclin D1 and CDK4 expression [3.68±0.01 (anti-miR-221/222) vs. 2.58±0.02 (anti-miR-221/222 + siANXA3) at 72 h timepoint; P<0.01; Fig. 5F].

Expression of ANXA3 is associated with chemotherapy sensitivity. After testing two concentrations of siANXA3 to reduce ANXA3 expression (Fig. 6A), the combined effects of doxorubicin and downregulation of ANXA3 were assessed in the MDA 231 cell line. In comparison with adriamycin alone, the combination of Adriamycin + siANXA3 significantly reduced cell viability in a dose-dependent manner (Fig. 6B). Anti-miR-221/222 therapy significantly reversed the enhanced chemosensitivity impact of siANXA3 compared with si-ANXA3 alone(Fig. 6C). Flow cytometry analysis of MDA 231 cells was used to confirm the inhibitory effect of ANXA3 downregulation on cell growth. Downregulation of ANXA3 increased the proportion of G_0/G_1 phase cells (50.8% vs. 55.5%) and decreased the S phase cell population (15.4% vs. 8.3%), according to cell cycle analyses (Fig. 6D). By contrast, alterations in ANXA3 expression did not notably influence the G_2/M phase cell population (22.5% vs. 22.3%; Fig. 6D). These findings may indicate that inhibiting cell proliferation by stopping cell cycle progression in the G_0/G_1 phase can be achieved by downregulating ANXA3 in breast cancer cells. FACS was performed using adriamycin 50 nM, which was selected based on the aforementioned viability data (Fig. 6B), to evaluate the effect of the combination of chemotherapy and siANXA3. By comparing the

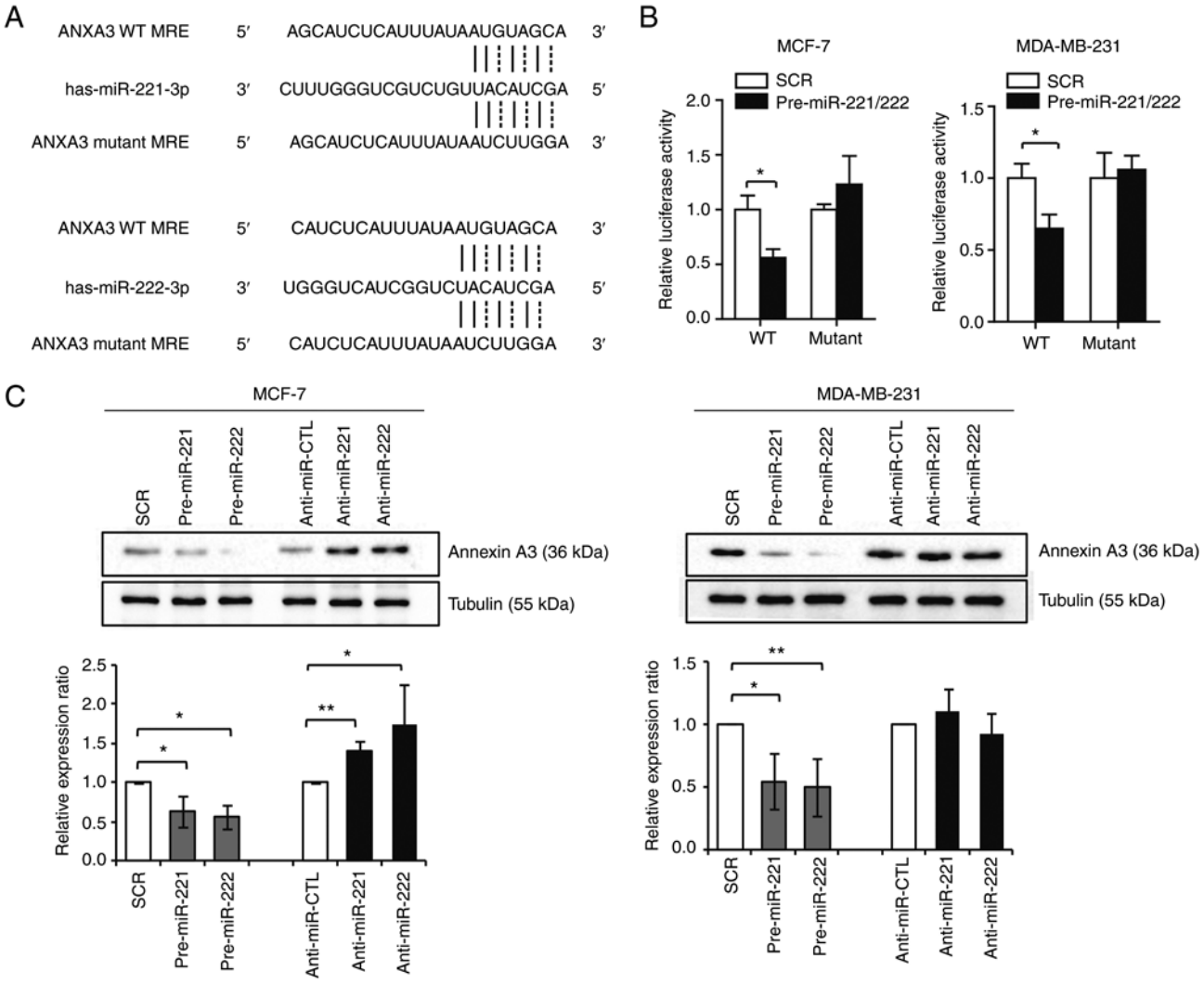

Figure 4. ANXA3 is a direct target of miR-221/222. (A) Predicted binding site of miR-221 and miR-222 in the 3'-UTR of WT and mutant ANXA3. (B) Luciferase activity was measured in MCF-7 and MDA-MB-231 cells after co-transfection with wild-type or mutant 3'-UTR of ANXA3 with pre-miR-221/222. (C) Differential expression of ANXA3 according to the transfection of control, pre-miR-221/222, anti-miR control and anti-miR-221/222. *P<0.05 and **P<0.01. MRE, miRNA recognition elements; ANXA3, annexin A3; miR, microRNA; SRC, scrambled negative control; WT, wild-type; anti-miR-CTL, anti-miR 221/222 negative control.

cell cycle analysis of cells treated with adriamycin alone and with the combination of Adriamycin + siANXA3, it was confirmed that siANXA3 on the G_0/G_1 arrest had an additional effect on G_2/M arrest induced by adriamycin (G_0/G_1, 20.9% vs. 32.6%; Fig. 6E). In the Adriamycin + siANX3 combination group, the expression levels of cyclin A and cyclin B1, which are the G_2/M checkpoint proteins, were reduced at all timepoints compared with the control. Cancer cells progression into the S phase was inhibited owing to a loss of cyclin D1 and CDK4 (Fig. 6F).

The apoptosis assay showed that treatment with siANXA3 alone exhibited similar apoptotic rates compared with the chemotherapy treatment [4.0±1.4 (control) vs. 11.0±6.1 (adriamycin) vs. 11.5±0.6% (siANXA3)] and confirmed the presence of additional effects in the combination siANXA3 + adriamycin (18.1±1.1%; Fig. 6G). In the western blotting, the levels of cleaved PARP and cleaved caspase 3 were also significantly increased in the combination group (Fig. 6H).

The survival analysis was performed using Kaplan-Meier Plotter software. ANXA3 expression was divided into two groups according to RNA gene chip results with the best cutoff value between the lower and upper quartiles. Notably, patients with breast cancer and higher ANXA3 expression had markedly reduced survival times relative to patients with low ANXA3 expression, especially in the basal-like subtype (Fig. 6I). Taken together, these findings revealed that a reduction in ANXA3 expression might increase the chemotherapy sensitivity by increasing G_0/G_1 arrest and apoptosis of cancer cells.

Discussion

MiR-221 and miR-222 expression levels vary in breast cancer according to tumor characteristics. The results of a previous study showed that the expression of miR-221 and miR-222 was increased in breast cancer tissues compared with normal breast tissues and high levels of miR-221 and miR-222 were associated with the advanced clinical stage of the tumor (19). In a subgroup analysis, miR-221 and miR-222 were shown to have a tendency of decreasing the expression of epithelial-specific

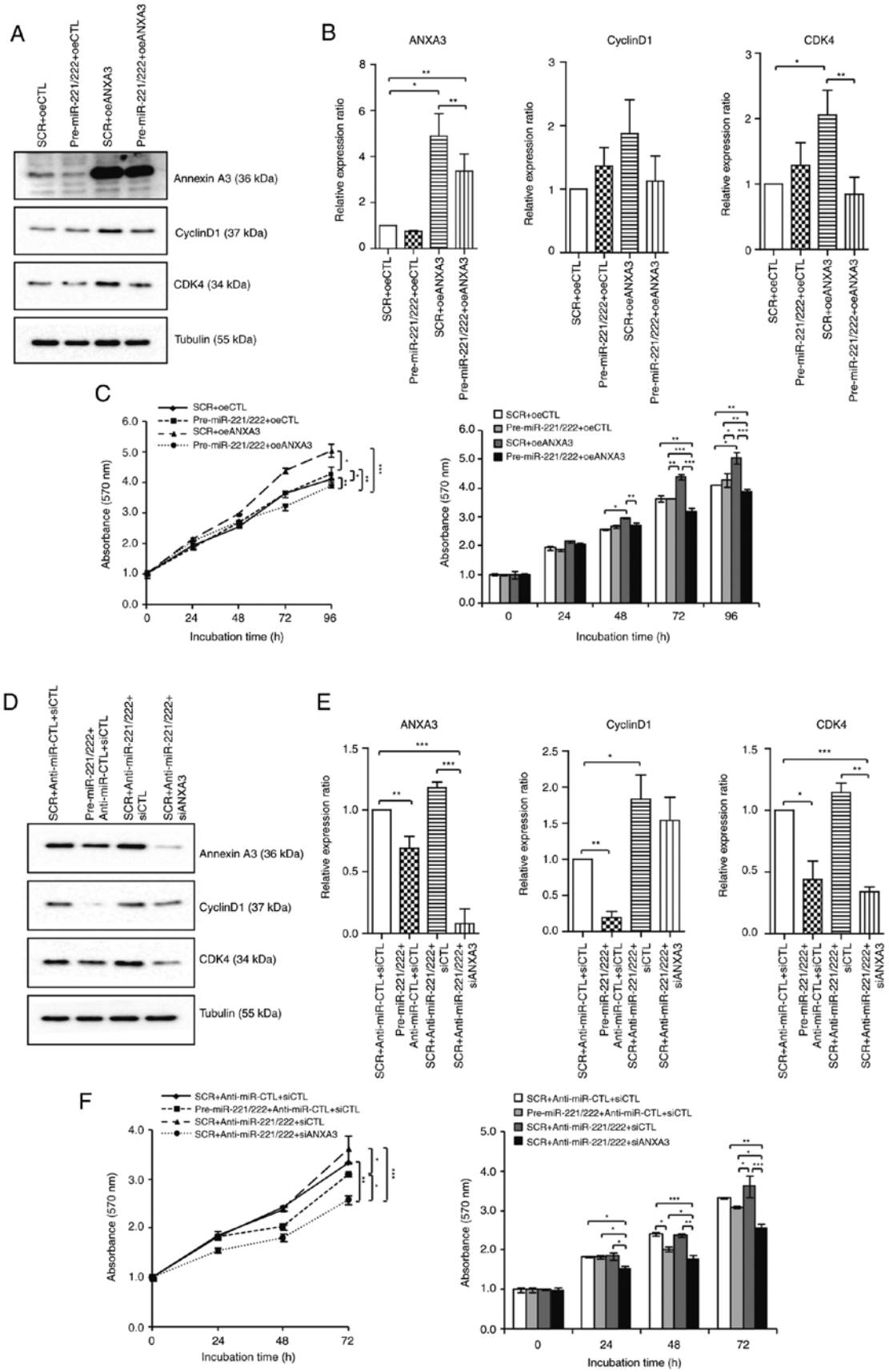

Figure 5. MiR-221/222 and ANXA3 axis regulates the cell cycle in breast cancer cell lines. Changes in the levels of cyclin D1 and CDK4 according to the miR-221/222 and ANXA3 axis in the MCF-7 cell line were examined using (A) western blotting and then (B) quantified. (C) Cell proliferation assays were performed after transfection of control, oeANXA3, miR-221/222 and combination treatment. Changes in the levels of cyclin D1 and CDK4 according to the miR-221/222 and ANXA3 axis in the MDA-MB-231 cell line were examined using (D) western blotting and then (E) quantified. (F) Cell proliferation assays were performed after transfection of control, inhibition of ANXA3, miR-221/222 and combination treatment. *P<0.05, **P<0.01 and ***P<0.001. ANXA3, annexin A3; SRC, scrambled negative control; oeCTL, overexpression negative control; oeANXA3, ANXA3 overexpression; siANXA3, small-interfering RNA targeting ANXA3; siCTL, small-interfering RNA negative control; miR, microRNA.

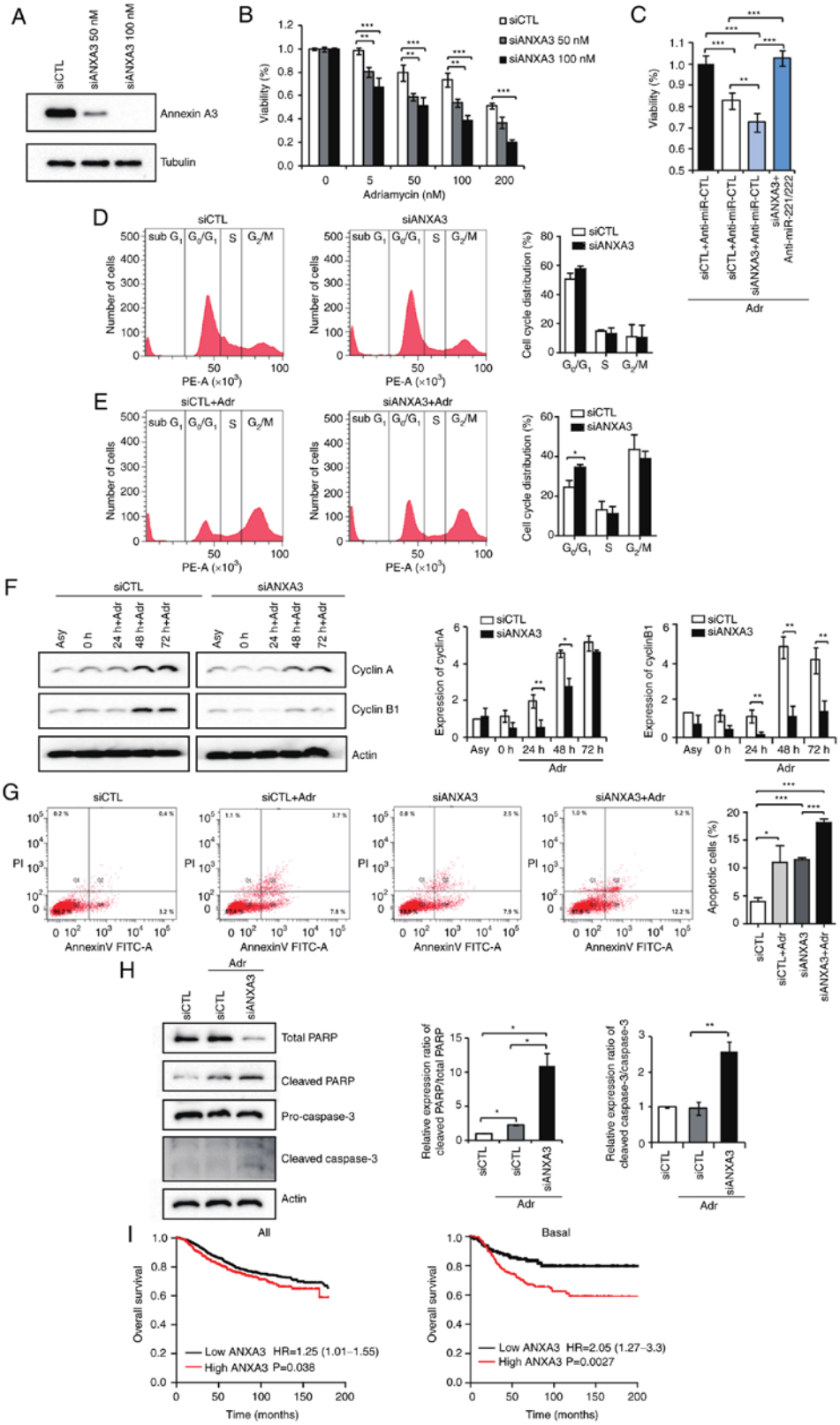

Figure 6. Expression of ANXA3 is associated with chemotherapy sensitivity. (A) Transfection efficiency was assessed according to siANXA3 concentration. (B) Cell viability was evaluated in MDA-MB-231 cells treated with si-ANXA3 and adriamycin at different doses. (C) Percentage of viable MDA-MB-231 cells. Cells were treated with adriamycin (25 nM), miR-221/222 and siANXA3. (D) Cell cycle profile was analyzed using flow cytometry. Fluorescence-activated cell sorting analysis of cells transfected with control or siANXA3. (E) FACS analysis of cells transfected with adriamycin (50 nM) alone or a combination of adriamycin and siANXA3. (F) Expression of two cell cycle regulatory factors, cyclin A and cyclin B1, were evaluated using western blotting after treatment with adriamycin alone and a combination of adriamycin and siANXA3. (G) Flow cytometry and annexin V-FITC/PI labeling were used to examine apoptosis after treatment with adriamycin, siANXA3 and their combination. (H) Expression of apoptotic factors was evaluated by western blotting after treatment with adriamycin alone and a combination of siANXA3. (I) Overall survival was evaluated according to ANXA3 levels using the Kaplan-Meier Plotter software. *P<0.05, **P<0.01 and ***P<0.001. ANXA3, annexin A3; FACS, fluorescence-activated cell sorting; Adr, adriamycin; SRC, scrambled negative control; siANXA3, small-interfering RNA targeting ANXA3; siCTL, small-interfering RNA negative control; Asy, asynchronous; PARP, poly (ADP-ribose) polymerase; anti-miR-CTL, anti-miR 221/222 negative control; miR, microRNA.

genes while increasing the expression of mesenchymal-specific genes, which is a property typical of the basal-like subtype (7). Furthermore, higher cell migratory affinity and invasiveness are associated with miR-221 and miR-222 expression, both of which are characteristics of the epithelial-mesenchymal transition (EMT) (7). In the present study, the expression levels of miR-221 and miR-222 were lower in the luminal type while higher in the basal type of breast cancer tissue compared with those in the normal breast tissue. From a clinical standpoint, miR-221 and miR-222 were associated with lymph node metastasis and disease recurrence, indicating them as potent prognosis markers.

The present study revealed that ANXA3 was a direct target of miR-221 and miR-222 in breast cancer. However, the expression of ANXA3 in the MDA-MB-231 cell line was originally high, so the effect of ANXA3 upregulation of anti-miR-221 and miR-222 was not visible in the western blotting analysis. For similar reasons, it can be considered that the effect of increasing the proliferation rate by transfection of anti-miR-221/222 in MDA-MB-231 cells also showed inconclusive results.

According to a previous study (14), the expression of ANXA3 is low in the MCF-7 cell line. Therefore, compared with the control, it is difficult to find a significant relationship between miR-221/222 transfection and the expression of cell cycle-related proteins. However, the miR-221/222 transfection in ANXA3 overexpressing MCF-7 cells was more effective in lowering ANXA3, cyclin D1 and CDK4 expression levels.

MiR-221/222 are considered to be important modulators of cancer progression that are involved in several aspects related to malignant tumors, such as cell invasion, metastasis, angiogenesis, apoptosis and drug resistance (6,9). In breast cancer cell lines, it has also been reported that miR-221/222 regulates EMT by targeting trichorhinophalangeal 1 (7) or adiponectin receptor 1 (20). Moreover, they have also been reported to promote cell cycle progression, migration and invasion by targeting cyclin-dependent kinase inhibitor 1B (21).

Cancer is considered a disease of cells with uncontrolled proliferation because cell proliferation is normally controlled with absolute fidelity by redundant regulatory pathways (22). Because CDKs are important for cell survival and death, their activity is tightly controlled (23). As a result, diverse regulatory systems for integrating external and internal information have emerged. The buildup and disappearance of cyclins dictate the functional intervals of CDKs. The cyclin D1 and CDK4/6 complex regulates cell cycle progression by phosphorylating and inactivating the retinoblastoma protein and associated proteins p107 and 130. Cyclin D1-CDK4/6-mediated phosphorylation of these proteins disables their negative regulatory role, allowing cells to progress from G_1 to the S phase (24). Furthermore, p16 acts as a CDK inhibitor, inactivating CDK4/6 and preventing Rb phosphorylation. Inactivation of p16 causes uncontrolled persistent Rb phosphorylation, which leads to the loss of cell cycle regulation (25). A recent study has revealed the role of miRNAs as regulators of the cell cycle; however, the exact functions still remain unclear because they may differ depending on the circumstance (26).

As a result of drug resistance, tumors often gain the ability to metastasize, resulting in serious consequences. Previous studies have revealed that miRNAs are involved in drug resistance (27-29). According to Rao *et al* (30), miR-221/222 regulate various oncogenic pathways, including catenin and transforming growth factor signaling mechanisms, which can promote fulvestrant resistance in breast cancer. By targeting PTEN and tissue inhibitors of metalloproteinase 3 tumor suppressors, Garofalo *et al* (31) discovered that miR-221/222 act as indicators of tumor necrosis factor-related apoptosis-inducing ligand sensitivity in lung cancer and hepatocellular carcinoma. MiR-21 is linked to acquired sorafenib resistance by decreasing autophagy via the Akt/PTEN pathway, according to the results of a similar study (32).

ANXA3 is a member of the annexin family that regulates cell development and plays a role in signal transduction pathways. In addition, it has been shown that ANXA3 is associated with chemotherapy resistance (33-35). Du *et al* (36) showed that the knockdown of ANXA3 increases the doxorubicin sensitivity of breast cancer cells by increasing the drug uptake. As a result, the combination treatment of ANXA3 with chemotherapeutic agents simultaneously inhibits tumor growth and metastasis *in vivo*. A neoadjuvant chemotherapeutic study of breast cancer has confirmed that inhibition of ANXA3 expression is associated with improved prognosis of patients (37).

There were several limitations in the present study, such as the small number of tissue samples used for the RT-qPCR analysis of miR-221 and miR-222 expression. Therefore, subgroup analyses according to breast cancer subtype and survival analyses according to the degree of expression of miR-221 and miR-222 were not performed. Moreover, the efficiency of siANXA3 showed a notable effect and inhibition of ANXA3 showed an inhibitory effect in cell proliferation by cyclin D1 and CDK4. So the combination effect of miR-221 and 222 to cell proliferation showed a small difference. However, several small molecule inhibitors lack specificity and can be associated with intolerable side effects and may have different *in vivo* efficiency. Nonetheless, the development of combined miR-221/222 and ANXA3-targeting-siRNA therapy allows for combined therapeutic targeting. Therefore, additional experiments are needed to confirm the combination effect through *in vivo* experiments.

The current study showed that miR-221/222 could negatively regulate cell proliferation through the inhibition of cell cycle progression in breast cancer by targeting ANXA3. Moreover, ANXA3 regulated the cell cycle by affecting the expression levels of cyclin D1 and CDK4 in breast cancer cells. In addition, the effects of ANXA3 can be increased or decreased by controlling the expression of miR-221/222, while ANXA3 downregulation showed an antitumor effect through cell cycle arrest. The present study evaluated the therapeutic potential of targeting the miR-221/222-ANXA3 axis. In combination with adriamycin, downregulation of ANXA3 may sensitize adriamycin-induced cell death through induction of persistent G_2/M and G_0/G_1 arrest. In conclusion, combining miR-221/222-induce ANXA3 regulation and chemotherapy could provide a promising therapeutic approach to inhibit tumor growth.

Acknowledgements

Not applicable.

Funding

The present study was supported by The Biomedical Research Institute Fund of Gyeongsang National University Hospital (grant no. GNUHBRIF-2019-0010) and a National Research Foundation of Korea grant sponsored by the Korean government (grant nos. NRF-2019R1F1A1057175 and NRF-2017R1D1A1B03034183).

Availability of data and materials

All data generated and/or analyzed during this study are included in this published article.

Authors' contributions

All authors made substantial contributions to the conception and design, acquisition of data, or analysis and interpretation of data. JYK, EJJ, JMK and YS designed the study. JMK and HSL analyzed the data. EJJ and YS performed the main experiments. SJK, JHP, JKC, HGK, CYJ, TP, SHJ and YTJ assisted in experiments, data analysis and discussion. JYK and EJJ confirm the authenticity of all the raw data. As the corresponding author, EJJ designed and coordinated the research and provided close guidance throughout the process. All authors read and approved the final manuscript.

Ethics approval and consent to participate

The Institutional Review Board of Gyeongsang National University Hospital approved the collection of breast tissue samples (approval no. GNUHIRB2009-54). Written informed consent was obtained from all the patients and all experimental protocols were approved by the Institutional Review Board of Gyeongsang National University Hospital.

Patient consent for publication

Not applicable.

Competing interests

The authors declare that they have no competing interests.

References

1. Saphner T, Tormey DC and Gray R: Annual hazard rates of recurrence for breast cancer after primary therapy. J Clin Oncol 14: 2738-2746, 1996.
2. Perou CM, Sørlie T, Eisen MB, van de Rijn M, Jeffrey SS, Rees CA, Pollack JR, Ross DT, Johnsen H, Akslen LA, *et al*: Molecular portraits of human breast tumours. Nature 406: 747-752, 2000.
3. Mohr AM and Mott JL: Overview of microRNA biology. Semin Liver Dis 35: 3-11, 2015.
4. Blenkiron C, Goldstein LD, Thorne NP, Spiteri I, Chin SF, Dunning MJ, Barbosa-Morais NL, Teschendorff AE, Green AR, Ellis IO, *et al*: MicroRNA expression profiling of human breast cancer identifies new markers of tumor subtype. Genome Biol 8: R214, 2007.
5. Iorio MV, Ferracin M, Liu CG, Veronese A, Spizzo R, Sabbioni S, Magri E, Pedriali M, Fabbri M, Campiglio M, *et al*: MicroRNA gene expression deregulation in human breast cancer. Cancer Res 65: 7065-7070, 2005.
6. Amini S, Abak A, Sakhinia E and Abhari A: MicroRNA-221 and microRNA-222 in common human cancers: Expression, function, and triggering of tumor progression as a key modulator. Lab Med 50: 333-347, 2019.
7. Stinson S, Lackner MR, Adai AT, Yu N, Kim HJ, O'Brien C, Spoerke J, Jhunjhunwala S, Boyd Z, Januario T, *et al*: miR-221/222 targeting of trichorhinophalangeal 1 (TRPS1) promotes epithelial-to-mesenchymal transition in breast cancer. Sci Signal 4: pt5, 2011.
8. Li B, Lu Y, Yu L, Han X, Wang H, Mao J, Shen J, Wang B, Tang J, Li C and Song B: miR-221/222 promote cancer stem-like cell properties and tumor growth of breast cancer via targeting PTEN and sustained Akt/NF-κB/COX-2 activation.. Chem Biol Interact 277: 33-42, 2017.
9. Abak A, Amini S, Sakhinia E and Abhari A: MicroRNA-221: biogenesis, function and signatures in human cancers. Eur Rev Med Pharmacol Sci 22: 3094-3117, 2018.
10. Li S, Li Q, Lü J, Zhao Q, Li D, Shen L, Wang Z, Liu J, Xie D, Cho WC, *et al*: Targeted inhibition of miR-221/222 promotes cell sensitivity to cisplatin in triple-negative breast cancer MDA-MB-231 cells. Front Genet 10: 1278, 2020.
11. Shen H, Lin Z, Shi H, Wu L, Ma B, Li H, Yin B, Tang J, Yu H and Yin X: MiR-221/222 promote migration and invasion, and inhibit autophagy and apoptosis by modulating ATG10 in aggressive papillary thyroid carcinoma. 3 Biotech 10: 339, 2020.
12. Tian F, Wang P, Lin D, Dai J, Liu Q, Guan Y, Zhan Y, Yang Y, Wang W, Wang J, *et al*: Exosome-delivered miR-221/222 exacerbates tumor liver metastasis by targeting SPINT1 in colorectal cancer. Cancer Sci 112: 3744-3755, 2021.
13. Liu C, Li N, Liu G and Feng X: Annexin A3 and cancer. Oncol Lett 22: 834, 2021.
14. Kim JY, Jung EJ, Park HJ, Lee JH, Song EJ, Kwag SJ, Park JH, Park T, Jeong SH, Jeong CY, *et al*: Tumor-suppressing effect of silencing of annexin A3 expression in breast cancer. Clin Breast Cancer 18: e713-e719, 2018.
15. Liu Q, Wang S, Pei G, Yang Y, Min X, Huang Y and Liu J: Impact analysis of miR-1253 on lung cancer progression through targeted regulation of ANXA3. Cancer Manag Res 13: 1767-1776, 2021.
16. Amin MB, Edge SB, Greene FL, Byrd DR, Brookland RK, Washington MK, Gershenwald JE, Compton CC, Hess KR, *et al*: AJCC Cancer Staging Manual. 8th edition. Springer, New York, NY, 2017.
17. Livak KJ and Schmittgen TD: Analysis of relative gene expression data using real-time quantitative PCR and the 2(-Delta Delta C(T)) method. Methods 25: 402-408, 2021.
18. He L, Du Z, Xiong X, Ma H, Zhu Z, Gao H, Cao J, Li T, Li H, Yang K, *et al*: Targeting androgen receptor in treating HER2 positive breast cancer. Sci Rep 7: 14584, 2017.
19. Eissa S, Matboli M, Sharawy A and El-Sharkawi F: Prognostic and biological significance of microRNA-221 in breast cancer. Gene 574: 163-167, 2015.
20. Hwang MS, Yu N, Stinson SY, Yue P, Newman RJ, Allan BB and Dornan D: MiR-221/222 targets adioponectin receptor 1 to promote the epithelial -to mesenchymal transition in breast cancer. PLoS One 11: e66502, 2013.
21. Li Y, Liang C, Ma H, Zhao Q, Lu Y, Xiang Z, Li L, Qin J, Chen Y, Cho WC, *et al*: miR-221/222 promotes S-phase entry and cellular migration in control of basal-like breast cancer. Molecules 30: 7122-7137, 2014
22. Harper JW and Adams PD: Cyclin-dependent kinases. Chem Rev 101: 2511-2526, 2001.
23. Malumbres M: Cyclin-dependent kinases. Genome Biol 15: 122, 2014.
24. Bertoli C, Skotheim JM and De Bruin RA: Control of cell cycle transcription during G1 and S phase. Nat Rev Mol Cell Biol 14: 518-528, 2013.
25. Kovatsi L, Georgiou E, Ioannou A, Haitoglou C, Tzimagiorgis G, Tsoukali H and Kouidou S: p16 promoter methylation in $Pb2^{+}$ -exposed individuals. Clin Toxicol (Phila) 48: 124-128, 2010.
26. Ghafouri-Fard S, Shoorei H, Anamag FT and Taheri M: The role of non-coding RNAs in controlling cell cycle related proteins in cancer cells. Front Oncol 30: 608975, 2020.
27. Mishra PJ: The miR-drug resistance connection: A new era of personalized medicine using noncoding RNA begins. Pharmacogenomics 13: 1321-1324, 2012.

28. Ma J, Dong C and Ji C: MicroRNA and drug resistance. Cancer Gene Ther 17: 523-531, 2010.
29. Zheng T, Wang J, Chen X and Liu L: Role of microRNA in anticancer drug resistance. Int J Cancer 126: 2-10, 2010.
30. Rao X, Di Leva G, Li M, Fang F, Devlin C, Hartman-Frey C, Burow ME, Ivan M, Croce CM and Nephew KP: MicroRNA-221/222 confers breast cancer fulvestrant resistance by regulating multiple signaling pathways. Oncogene 30: 1082-1097, 2011.
31. Garofalo M, Di Leva G, Romano G, Nuovo G, Suh SS, Ngankeu A, Taccioli C, Pichiorri F, Alder H, Secchiero P, *et al*: miR-221&222 regulate trail resistance and enhance tumorigenicity through PTEN and TIMP3 downregulation. Cancer Cell 16: 498-509, 2009.
32. He C, Dong X, Zhai B, Jiang X, Dong D, Li B, Jiang H, Xu S and Sun X: MiR-21 mediates sorafenib resistance of hepatocellular carcinoma cells by inhibiting autophagy via the PTEN/Akt pathway. Oncotarget 6: 28867-28881, 2015.
33. Yan X, Yin J, Yao H, Mao N, Yang Y and Pan L: Increased expression of annexin A3 is a mechanism of platinum resistance in ovarian cancer. Cancer Res 70: 1616-1624, 2010.
34. Tong SW, Yang YX, Hu HD, An X, Ye F, Hu P, Ren H, Li SL and Zhang DZ: Proteomic investigation of 5-fluorouracil resistance in a human hepatocellular carcinoma cell line. J Cell Biochem 113: 1671-1680, 2012.
35. Pénzváltó Z, Tegze B, Szász AM, Sztupinszki Z, Likó I, Szendrői A, Schäfer R and Győrffy B: Identifying resistance mechanisms against five tyrosine kinase inhibitors targeting the ERBB/RAS pathway in 45 cancer cell lines. PLoS One 8: e59503, 2013.
36. Du R, Liu B, Zhou L, Wang D, He X, Xu X, Zhang L, Niu C and Liu S: Downregulation of annexin A3 inhibits tumor metastasis and decreases drug resistance in breast cancer. Cell Death Dis 9: 126, 2018.
37. Zhu S, Li Y, Wang Y, Cao J, Li X, Wang J and Wang X: Efficacy of neoadjuvant chemotherapy and annexin A3 expression in breast cancer. J BUON 24: 522-528, 2019.